The Chicxulub Asteroid Impact and Mass Extinction at the Cretaceous-Paleogene Boundary

Peter Schulte,[1]* Laia Alegret,[2] Ignacio Arenillas,[2] José A. Arz,[2] Penny J. Barton,[3] Paul R. Bown,[4] Timothy J. Bralower,[5] Gail L. Christeson,[6] Philippe Claeys,[7] Charles S. Cockell,[8] Gareth S. Collins,[9] Alexander Deutsch,[10] Tamara J. Goldin,[11] Kazuhisa Goto,[12] José M. Grajales-Nishimura,[13] Richard A. F. Grieve,[14] Sean P. S. Gulick,[6] Kirk R. Johnson,[15] Wolfgang Kiessling,[16] Christian Koeberl,[11] David A. Kring,[17] Kenneth G. MacLeod,[18] Takafumi Matsui,[19] Jay Melosh,[20] Alessandro Montanari,[21] Joanna V. Morgan,[9] Clive R. Neal,[22] Douglas J. Nichols,[15] Richard D. Norris,[23] Elisabetta Pierazzo,[24] Greg Ravizza,[25] Mario Rebolledo-Vieyra,[26] Wolf Uwe Reimold,[16] Eric Robin,[27] Tobias Salge,[28] Robert P. Speijer,[29] Arthur R. Sweet,[30] Jaime Urrutia-Fucugauchi,[31] Vivi Vajda,[32] Michael T. Whalen,[33] Pi S. Willumsen[32]

The Cretaceous-Paleogene boundary ~65.5 million years ago marks one of the three largest mass extinctions in the past 500 million years. The extinction event coincided with a large asteroid impact at Chicxulub, Mexico, and occurred within the time of Deccan flood basalt volcanism in India. Here, we synthesize records of the global stratigraphy across this boundary to assess the proposed causes of the mass extinction. Notably, a single ejecta-rich deposit compositionally linked to the Chicxulub impact is globally distributed at the Cretaceous-Paleogene boundary. The temporal match between the ejecta layer and the onset of the extinctions and the agreement of ecological patterns in the fossil record with modeled environmental perturbations (for example, darkness and cooling) lead us to conclude that the Chicxulub impact triggered the mass extinction.

Paleontologists have long recognized the global scale and abruptness of the major biotic turnover at the Cretaceous-Paleogene (K-Pg, formerly K-T) boundary ~65.5 million years ago (Ma). This boundary represents one of the most devastating events in the history of life (*1*) and abruptly ended the age of the dinosaurs. Thirty years ago, the discovery of an anomalously high abundance of iridium and other platinum group elements (PGEs) in the K-Pg boundary clay led to the hypothesis that an asteroid ~10 km in diameter collided with Earth and rendered many environments uninhabitable (*2*, *3*).

The occurrence of an impact is substantiated by the recognition of impact ejecta including spherules, shocked minerals, and Ni-rich spinels in many K-Pg boundary event deposits [e.g., (*4*, *5*)]. The ejecta distribution points to an impact event in the Gulf of Mexico–Caribbean region; this prediction is reinforced by the discovery of the ~180- to 200-km-diameter Chicxulub crater structure on the Yucatan peninsula, Mexico (*6*). Modeling suggests that the size of the crater and the release of climatically sensitive gases from the carbonate- and sulfate-rich target rocks could have caused catastrophic environmental effects such as extended darkness, global cooling, and acid rain (*7*–*9*). These effects provide an array of potential mechanisms for the ecologically diverse but selective abrupt extinctions (Fig. 1) (*10*–*13*).

Notwithstanding the substantial evidence supporting an impact mechanism, other interpretations of the K-Pg boundary mass extinction remain. Stratigraphic and micropaleontological data from the Gulf of Mexico and the Chicxulub crater have instead been used to argue that this impact preceded the K-Pg boundary by several hundred thousand years and therefore could not have caused the mass extinction [e.g., (*14*)]. In addition, the approximately one-million-year-long emplacement of the large Deccan flood basalts in India spans the K-Pg boundary (Fig. 1); the release of sulfur and carbon dioxide during these voluminous eruptions may have caused severe environmental effects (*15*) that have also been proposed as triggers for the mass extinction at the K-Pg boundary (*16*).

Here, we assess the observational support for these divergent interpretations by synthesizing recent stratigraphic, micropaleontological, petrological, and geochemical data from the globally distributed K-Pg boundary event deposit. Impact and volcanism as extinction mechanisms are evaluated in terms of their predicted environmental perturbations and, ultimately, the distribution of life on Earth before and after the K-Pg boundary.

What Is the Evidence for Correlating the Impact with the K-Pg Boundary?

The Upper Cretaceous and lower Paleogene sediments bracketing the K-Pg boundary event deposits are among the most intensively investigated deposits in the geological record. More than 350 K-Pg boundary sites are currently known, and these sites show a distinct ejecta distribution pattern related to distance from the Chicxulub crater (Fig. 2 and table

[1]GeoZentrum Nordbayern, Universität Erlangen-Nürnberg, Schlossgarten 5, D-91054 Erlangen, Germany. [2]Departamento de Ciencias de la Tierra e Instituto Universitario de Investigación de Ciencias Ambientales de Aragón, Universidad de Zaragoza, Pedro Cerbuna 12, E-50009 Zaragoza, Spain. [3]Department of Earth Sciences, University of Cambridge, Cambridge CB2 3EQ, UK. [4]Department of Earth Sciences, University College London, Gower Street, London WC1E 6BT, UK. [5]Department of Geosciences, Pennsylvania State University, University Park, PA 16802, USA. [6]Institute for Geophysics, Jackson School of Geosciences, University of Texas at Austin, J.J. Pickle Research Campus, 10100 Burnet Road 196-ROC, Austin, TX 78759, USA. [7]Earth System Science, Vrije Universiteit Brussel, Pleinlaan 2, B-1050 Brussels, Belgium. [8]Centre for Earth, Planetary, Space and Astronomical Research, Open University, Milton Keynes MK7 6AA, UK. [9]Earth Science and Engineering, Imperial College London, London SW7 2BP, UK. [10]Institut für Planetologie, Universität Münster, D-48149 Münster, Germany. [11]Department of Lithospheric Research, University of Vienna, Althanstrasse 14, A-1090 Vienna, Austria. [12]Tsunami Engineering Laboratory, Disaster Control Research Center, Graduate School of Engineering, Tohoku University, 6-6-11-1106 Aoba, Aramaki, Sendai 980-8579, Japan. [13]Programa de Geología de Exploracíon y Explotacíon, Dirección de Investigación y Posgrado, Instituto Mexicano del Petróleo, Eje Lázaro Cárdenas No. 152, C.P. 07730, México City, México. [14]Earth Sciences Sector, Natural Resources Canada, Ottawa, Ontario K1A 0E4, Canada. [15]Research and Collections Division, Denver Museum of Nature and Science, 2001 Colorado Boulevard, Denver, CO 80205, USA. [16]Museum für Naturkunde, Leibniz Institute at the Humboldt University Berlin, Invalidenstrasse 43, D-10115 Berlin, Germany. [17]Center for Lunar Science and Exploration, Universities Space Research Association–Lunar and Planetary Institute, 3600 Bay Area Boulevard, Houston, TX 77058–1113, USA. [18]Department of Geological Sciences, University of Missouri, Columbia, MO 65211, USA. [19]Planetary Exploration Research Center, Chiba Institute of Technology, 2-17-1 Tsudanuma, Narashino, Chiba 275-0016, Japan. [20]Earth and Atmospheric Sciences, Purdue University, 550 Stadium Mall Drive, West Lafayette, IN 47907–2051, USA. [21]Osservatorio Geologico di Coldigioco, 62021 Apiro (MC), Italy. [22]Department of Civil Engineering and Geological Sciences, 156 Fitzpatrick Hall, University of Notre Dame, Notre Dame, IN 46556, USA. [23]SIO Geological Collections, 301 Vaughan Hall, MS-0244, Scripps Institution of Oceanography, La Jolla, CA 92093–0244, USA. [24]Planetary Science Institute, 1700 East Fort Lowell Road, Suite 106, Tucson, AZ 85719, USA. [25]Department of Geology and Geophysics, School of Ocean and Earth Science and Technology, University of Hawaii, Manoa, Honolulu, HI 96822, USA. [26]Unidad de Ciencias del Agua, Centro de Investigación Científica de Yucatán, A.C., Calle 8, No. 39, Mz. 29, S.M. 64, Cancún, Quintana Roo, 77500, México. [27]Laboratoire des Sciences du Climat et de l'Environnement, Institut Pierre et Simon Laplace, Commission à l'Énergie Atomique/CNRS/Université de Versailles Saint Quentin en Yveunes–UMR 1572, Avenue de la Terrasse, F-91198 Gif-sur-Yvette Cedex, France. [28]Bruker Nano GmbH, Schwarzschildstraße 12, D-12489 Berlin, Germany. [29]Department of Earth and Environmental Sciences, K.U.Leuven, Box 2408, Celestijnenlaan 200E, 3001 Leuven, Belgium. [30]Natural Resources Canada, Geological Survey of Canada Calgary, 3303 33rd Street NW, Calgary, AB T2L 2A7, Canada. [31]Laboratorio de Paleomagnetismo y Paleoambientes, Programa Universitario de Perforaciones en Oceanos y Continentes, Instituto de Geofísica, Universidad Nacional Autónoma de México (UNAM), DF 04510 Mexico, Mexico. [32]Department of Earth and Ecosystem Sciences, Lund University, Sölvegatan 12, 223 62 Lund, Sweden. [33]Department of Geology and Geophysics, University of Alaska, Fairbanks, AK 99775, USA.

*To whom correspondence should be addressed. E-mail: schulte@geol.uni-erlangen.de. The remaining authors contributed equally to this work.

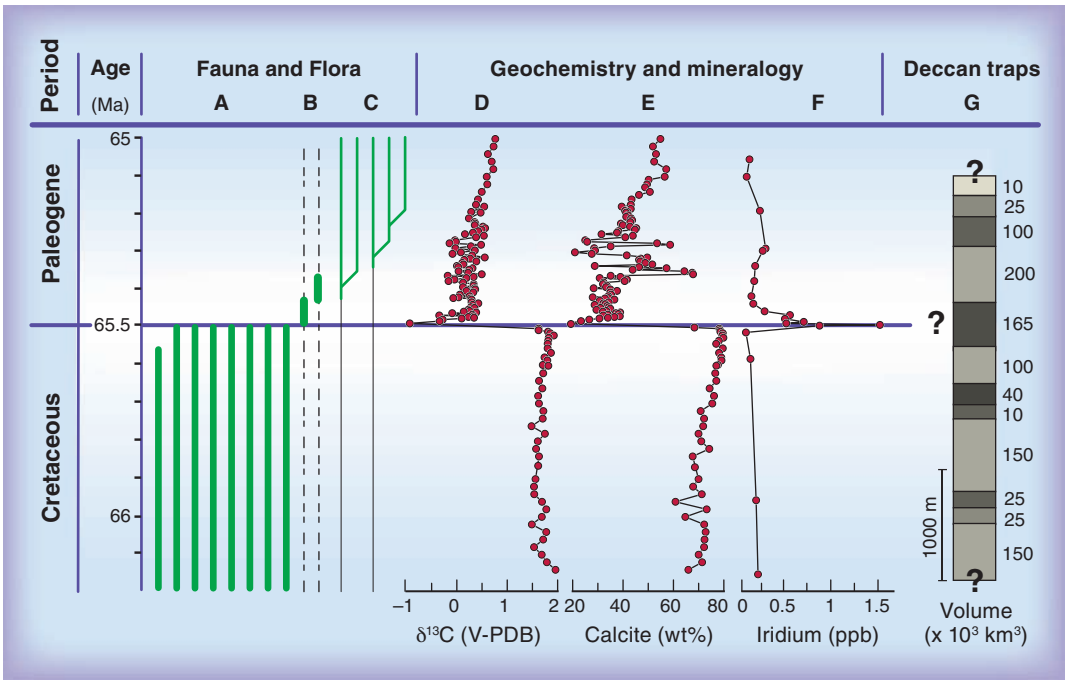

Fig. 1. Stratigraphy and schematic record of biotic events across the K-Pg boundary correlated to the chemical and mineralogical records of a core from the North Atlantic [Ocean Drilling Program (ODP) Leg 207] and the major eruptive units of the Deccan flood basalt province, India. Many (>60%) Cretaceous species experienced mass extinction at the boundary (A), whereas successive blooms of opportunistic species (B) and radiation of new species (C) occurred in the Early Paleogene. V-PDB indicates the Vienna Pee Dee Belemnite; wt %, weight %; and ppb, parts per billion. The mass extinction coincides with a major perturbation of the global carbon cycle as indicated by a negative $\delta^{13}C$ anomaly (D), a major drop of carbonate sedimentation in the marine realm (E), and the enrichment of PGEs in Chicxulub ejecta deposits (F) (*25*, *26*). Composite stratigraphic column of the formations of the main Deccan Trap flood basalt province showing their cumulative thickness and estimated basalt volumes (G) (*15*). Note that the exact stratigraphic onset and end of the main Deccan flood basalt sequence and the precise position of the K-Pg boundary in the formations have yet to be determined, as indicated by the question marks (*16*). However, the onset of the main eruption phase is ~400 to 600 thousand years before the K-Pg boundary as is also shown by Os isotope data (*38*).

S1) (*17*, *18*). Accordingly, the K-Pg boundary sites can be divided into four groups (Fig. 2 and table S1): (i) In very proximal settings up to 500 km from Chicxulub, impact deposits are quite thick. Cores recovered close to the crater rim inside the Chicxulub impact structure include a >100-m-thick impact-breccia sequence, and 1-m- to >80-m-thick ejecta-rich deposits are present in the surrounding Central American region [e.g., (*19*–*21*)]. (ii) In proximal areas around the northwestern Gulf of Mexico from 500 to 1000 km from Chicxulub, the K-Pg boundary is characterized by a series of cm- to m-thick ejecta spherule-rich, clastic event beds indicative of high-energy sediment transport, for example, by tsunamis and gravity flows (*18*, *22*, *23*). (iii) At intermediate distances from Chicxulub (~1000 to ~5000 km), the K-Pg boundary deposit consists of a 2- to 10-cm-thick spherule layer topped by a 0.2- to 0.5-cm-thick layer anomalously rich in PGEs with abundant shocked minerals, granitic clasts, and Ni-rich spinels (Fig. 3) (*12*, *24*–*26*). (iv) In distal marine sections more than 5000 km from Chicxulub, a reddish, 2- to 5-mm-thick clay layer rich in impact ejecta material is usually present at the K-Pg boundary [e.g., (*17*)]. The bedding plane between the impact-ejecta-rich red clay layer and the underlying Cretaceous marls coincident with the abrupt mass extinction in the El Kef section, Tunisia, is also the officially defined base of the Paleogene (fig. S1) (*27*). This definition implies that the impact-generated sediments in the K-Pg boundary interval stratigraphically belong to the Paleogene (Fig. 2).

The pattern of decreasing ejecta-layer thickness with increasing distance from the impact crater is consistent with the Chicxulub impact as the unique source for the ejecta in the K-Pg boundary event deposit (Figs. 2 and 3 and table S1). Additional support for this genetic link derives from the distribution, composition, and depositional mode of the ejecta. First, the size and abundance of spherules and ballistically ejected shocked quartz grains, which are resistant to alteration, decrease with increasing distance from Chicxulub (*18*, *28*). Second, the specific composition [e.g., silicic spherules, shocked limestone, and dolomite and granitic clasts (Fig. 3 and figs. S2 to S4)] (*29*) and age distribution (table S2) of the ejecta match the suite of Chicxulub target rocks. Lastly, the presence of the high-energy clastic unit at proximal K-Pg boundary sites, intercalated between two layers rich in Chicxulub ejecta, suggests that the Chicxulub impact caused a collapse of the Yucatan carbonate platform and triggered mass flows and tsunamis in the Gulf of Mexico and adjacent areas (Fig. 2 and figs. S3 to S8) (*17*, *18*, *30*). Therefore, the K-Pg boundary clastic unit, up to 80 m thick in places, was deposited in the extremely brief period between the arrival of coarse-grained spherules and the subsequent, longer-term deposition of the finer-grained PGE- and Ni-rich ejecta phases (Fig. 2) (*22*).

A contrasting hypothesis is founded on the interpretation that the clastic unit is a long-term depositional sequence genetically unrelated to the Chicxulub impact event (*14*, *31*); lenslike spherule deposits locally present below the clastic unit in Mexico would then correlate to the base of the uppermost Cretaceous planktic foraminiferal zone (*14*, *31*). This interpretation also proposes a latest Cretaceous age for the impact breccia found within the Chicxulub crater with the implication that all intermediate to distal K-Pg boundary sites lack the resolution and completeness to firmly establish a correlation to the Chicxulub impact event (*14*, *32*). Additionally, the assertion that the Chicxulub impact preceded the K-Pg mass extinction by ~300 thousand years predicts that the PGE anomaly at the top of the clastic unit resulted from a second large impact event (*14*). In this scenario, either the second impact event or the Deccan flood basalt eruptions caused the K-Pg mass extinction (*14*).

However, sedimentological and petrological data suggest that the lenslike ejecta deposits in Mexico were generated by impact-related liquefaction and slumping, consistent with the single very-high-energy Chicxulub impact (figs. S5 to S9) (*23*). A range of sedimentary structures and the lack of evidence for ocean floor colonization within the clastic unit in northeastern Mexico indicate rapid deposition (figs. S6 to S8) (*22*, *23*). Moreover, the presence of shallow-water benthic foraminifera in the clastic unit (*33*) contradicts a long-term depositional sequence (*14*); if in situ, their presence requires unrealistically rapid relative sea-level changes of >500 m. Lastly, high-resolution planktic foraminiferal analyses in the southern Mexican sections demonstrate that the Chicxulub-linked clastic unit is biostratigraphically equivalent to the officially defined base of the Paleocene (i.e., the red clay

layer) in the El Kef section, Tunisia (Fig. 2 and fig. S1) (*20*).

A pre–K-Pg boundary age for the Chicxulub event has also been argued on the basis of the sequence at a Brazos River site in Texas and from within the crater. If a 3-cm-thick clay layer interbedded in Upper Cretaceous shales at the Brazos River site originated from the Chicxulub impact, the impact occurred significantly before the K-Pg boundary (*31*). Yet, in this clay layer there are no spherules or shocked minerals that would provide evidence for an impact origin, and its high sanidine and quartz content supports a local volcanic origin similar to ash layers found below the K-Pg boundary in Mexico and Haiti (table S3 and figs. S10 to S12).

Within the Chicxulub crater, an ~50-cm-thick dolomitic sandstone unit between the impact breccias and the lower Paleocene postimpact crater infill has been interpreted as undisturbed sediments deposited immediately after the impact (fig. S13) (*32*). Rare uppermost Cretaceous planktic foraminifera within this unit were proposed as evidence that the impact preceded the K-Pg mass extinction (*32*). However, this sandstone unit is in part cross-bedded, contains ejecta clasts (fig. S14), and also includes planktic foraminifera of Early Cretaceous age (figs. S14 and S15) (*34*, *35*). These observations, as well as grain-size data (*36*), indicate that deposition of this sequence was influenced by erosion and reworking after the impact and therefore provide no evidence for a long-term postimpact and pre–K-Pg boundary deposition.

In addition, multiple independent lines of evidence place the Chicxulub event at the K-Pg boundary. Geochronologic data demonstrate that the Chicxulub impact correlates to the K-Pg boundary at ~65.5 Ma (*29*). Detailed investigation of continuous sequences from globally distributed marine and terrestrial sites yield no chemical or physical evidence of a large impact in the last million years of the Cretaceous other than the Chicxulub event (table S1 and fig. S16) (*25*, *37*, *38*). Lastly, orbital cycles in deep-sea sites [(*39*) and references therein] demonstrate that there is neither a proposed global 300-thousand-year gap (*14*) nor a hiatus between the Chicxulub impact and the K-Pg boundary.

What Were the Initial Consequences of the Impact?

Asteroid impact models [e.g., (*40*)] predict that an impact large enough to generate the Chicxulub crater would induce earthquakes (magnitude > 11), shelf collapse around the Yucatan platform, and widespread tsunamis sweeping the coastal zones of the surrounding oceans (*7*). Moreover, models suggest the Chicxulub impact had sufficient energy to eject and distribute material around the globe (*7*), possibly enhanced by decomposition of the volatile-rich carbonate and sulfate sediments (*41*). Near-surface target material was ejected ballistically at velocities up to a few km/s as part of the ejecta curtain. This yielded the thick spherule layer at proximal sites and the basal spherule layer at intermediate distance sites (Fig. 2) (*41*). Parts of the ejecta would be entrained within the impact plume: a complex mixture of hot air;

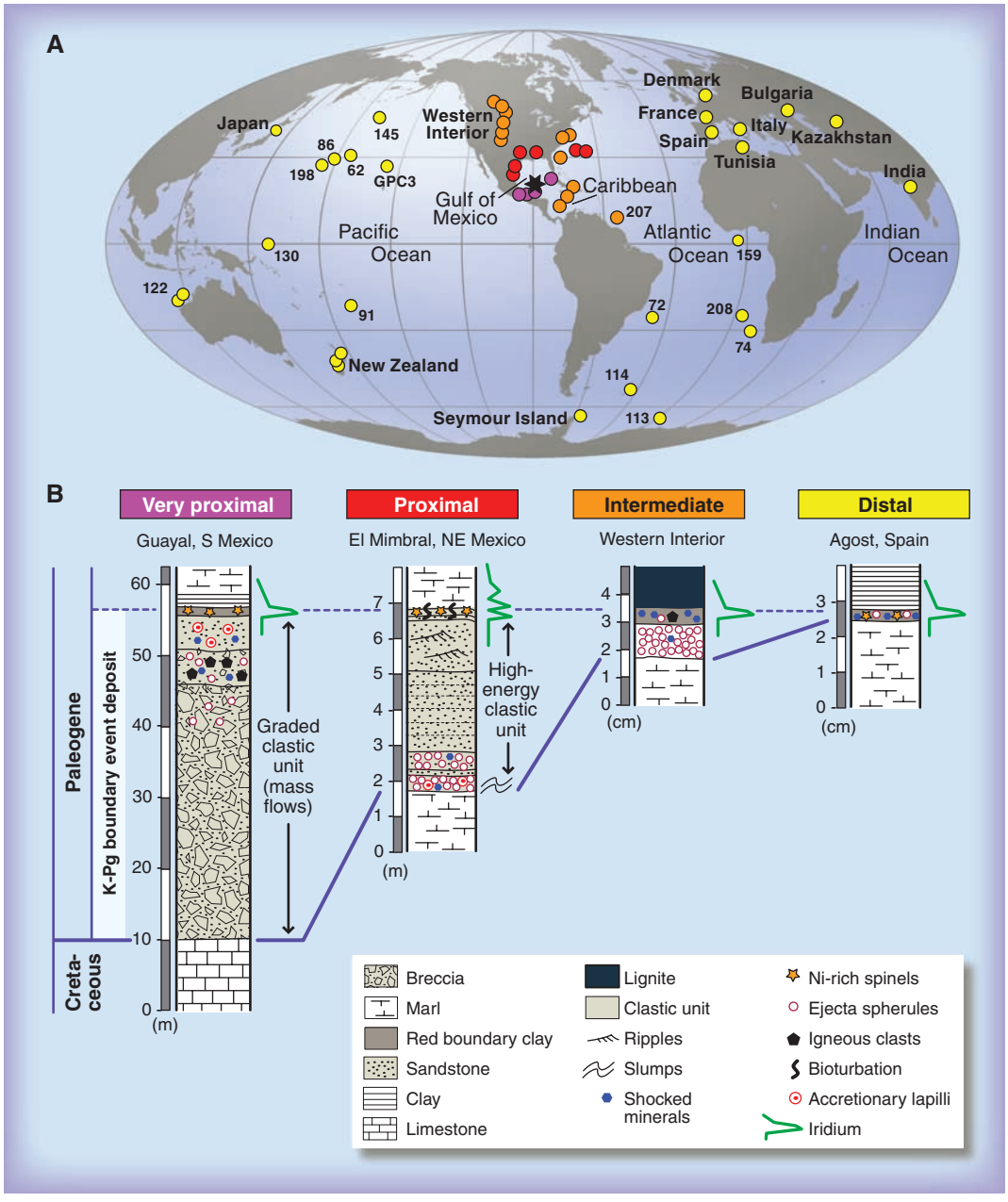

Fig. 2. (**A**) Global distribution of key K-Pg boundary locations. Deep-Sea drill sites are referred to by the corresponding Deep Sea Drilling Project (DSDP) and ODP Leg numbers. The asterisk indicates the location of the Chicxulub impact structure. Colored dots mark the four distinct types of K-Pg boundary event deposit related to distance from the Chicxulub crater (table S1): magenta, very proximal (up to 500 km); red, proximal (up to 1000 km); orange, intermediate distance (1000 to 5000 km); and yellow, distal (>5000 km). Schematic lithologs of the four groups of K-Pg boundary event deposits (**B**) highlighting high-energy event beds (clastic unit) proximal to the crater and the depositional sequence of different materials that originated in one single impact in proximal to distal sites.

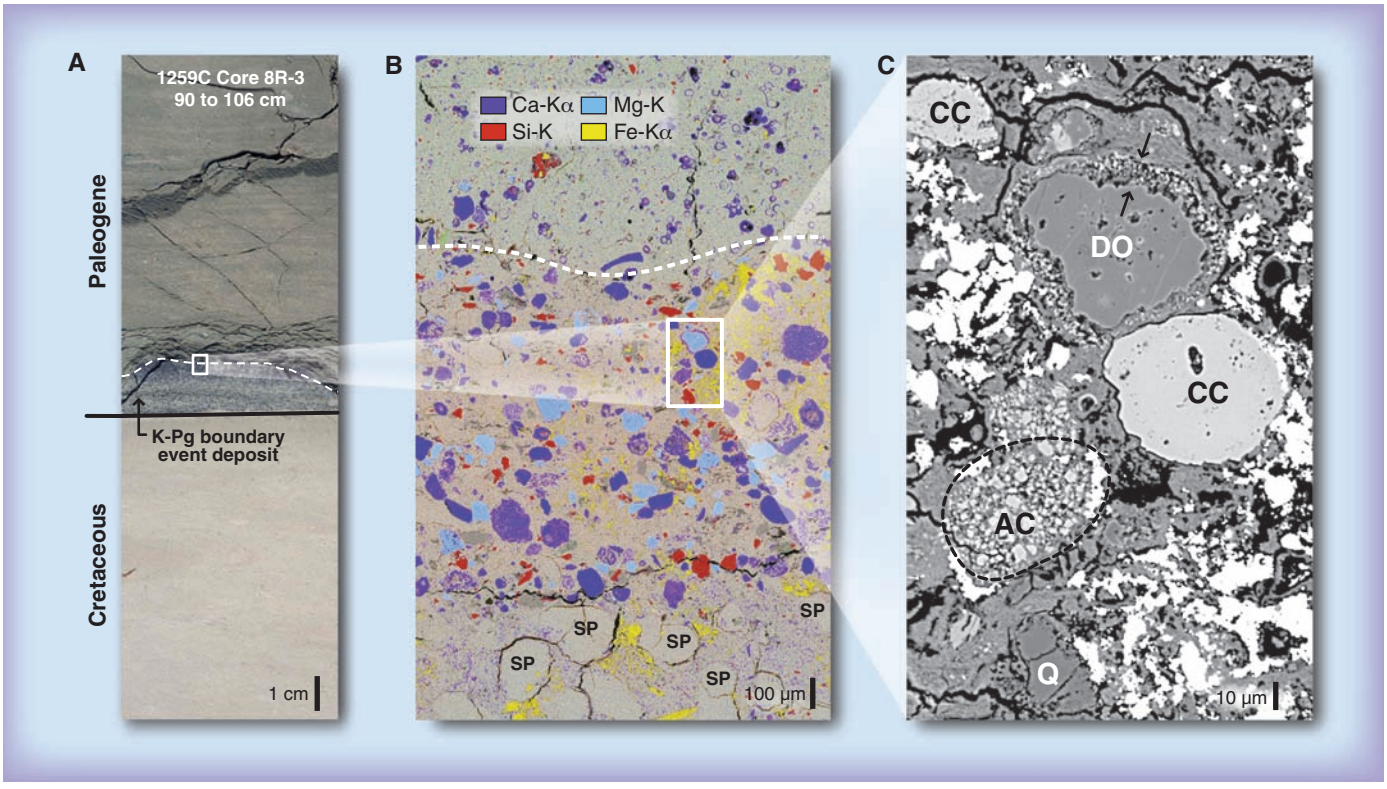

Fig. 3. The K-Pg boundary at ODP Leg 207, western North Atlantic (**A**). An energy-dispersive element distribution map of the box in (A) shows the transition from the top of the spherule-rich graded ejecta sequence (SP) to the lowermost Paleogene sediments (**B**). Note abundant calcite (blue) and dolomite (turquoise) ejecta material as well as occurrence of shocked quartz grains (red) in the uppermost 0.5 mm. A backscattered electron image of the box in (B) shows a rounded dolomite clast (DO) with a Ca-rich clay shell (between arrows), a rounded calcite clast (CC), an accretionary calcite clast (AC), and quartz (Q) interpreted to be of shock-metamorphic origin resulting from the Chicxulub impact (**C**).

projectile material; and impact-vaporized, shock-melted, and fragmented target rocks that expanded rapidly by several km/s up to velocities greater than Earth's escape velocity of 11 km/s. Projectile-rich impact plume deposits form the upper layer in intermediate-distance K-Pg sections and contribute to the single red K-Pg boundary clay layer at distal sites, enriching both in PGEs and shocked minerals (Fig. 2).

Detailed multiphase flow models suggest that the atmospheric reentry of the ejecta spherules may have caused a global pulse of increased thermal radiation at the ground (*42*). Such a thermal pulse is below the lower limits of woody biomass ignition, in agreement with studies yielding no evidence for widespread large wildfires at the K-Pg boundary (*43*), with a possible exception for the Gulf of Mexico region close to the impact site [(*9*) and references therein]. However, the modeled level of radiation is expected to have resulted in thermal damage to the biosphere even if the maximum radiation intensity was only sustained for a few minutes.

Geophysical models indicate that the impact release of large quantities of water, dust, and climate-forcing gases would dramatically alter the climate system (*7*, *8*). The estimated amount of the silicic sub-micrometer-sized dust input of 0.01 to 0.1 Gt (1 Gt = 10^{15}g) is considered to be too low by itself to cause a catastrophic impact winter (*44*). However, abundant sub-micrometer-sized particulate carbonates in the ejecta (*26*) and soot, a strong absorber of short-wave radiation, derived from burning of targeted carbonaceous sediments may have greatly amplified the effects of dust injection (*43*). In addition, there are estimates of at least 100 to 500 Gt of sulfur released nearly instantaneously (*7*, *8*). These figures are likely to be conservative given new larger estimates of the volume of water and sulfur-bearing sediments within Chicxulub's 100-km-diameter transient crater (*45*). The sulfur was probably rapidly transformed to sunlight-absorbing sulfur aerosols with the capacity to cool Earth's surface for years to decades by up to 10°C (*8*, *10*). Temperatures of the deep ocean, however, remained largely unaffected by the impact because of the ocean's large thermal mass (*46*), contributing to a rapid recovery of the global climate. The sulfur release also generated acid rain, which, although not sufficient to completely acidify ocean basins, would have severely affected marine surface waters and/or poorly buffered continental catchments and watersheds (*9*).

Although current models cannot fully assess the combined environmental consequences of the Chicxulub impact (*7*, *9*), the extremely rapid injection rate of dust and climate-forcing gases would have magnified the environmental consequences compared with more-prolonged volcanic eruptions, particularly when compounded by the additional adverse effects of a large impact (e.g., heat wave, soot, and dust release) that are absent during flood basalt volcanism. Specifically, the injection of ~100 to 500 Gt of sulfur into the atmosphere within minutes after the Chicxulub impact contrasts with volcanic injection rates of 0.05 to 0.5 Gt of sulfur per year during the ~1-million-year-long main phase of Deccan flood basalt volcanism (Fig. 1 and fig. S16) (*15*, *16*). Indeed, an only moderate climate change (~2°C warming) during the last 400 thousand years of the Cretaceous has been interpreted to result from Deccan flood basalt volcanism [e.g., (*47*)].

What Does the Fossil Record Reveal About the Global Consequences for Life?

The scale of biological turnover between the Cretaceous and Paleogene is nearly unprecedented in Earth history (*1*). A number of major animal groups disappeared across the boundary (e.g., the nonavian dinosaurs, marine and flying reptiles, ammonites, and rudists) (*48*), and several other major groups suffered considerable, but not complete, species-level extinction (e.g., planktic foraminifera, calcareous nannofossils, land plants) (*12*, *13*, *37*, *49*). Even the groups that showed negligible extinctions exhibited substantial changes in assemblage composition (e.g., benthic foraminifera) (*50*).

For marine phytoplankton, major drivers of ocean productivity, darkness, and suppression of photosynthesis were likely major killing

mechanisms (*9*). There is a clear separation in extinction rate between strongly affected phytoplankton groups with calcareous shells and groups that had organic or siliceous shells. Although the possible effects of surface ocean acidification after the impact may have been an additional stress factor, this selectivity seems to have favored traits contributing to survival of acute stress (*11*, *13*). For example, cyst-forming dinoflagellates persisted through the K-Pg boundary, although assemblage changes suggest a brief cooling phase after the impact [(*51*) and references therein].

The extinction of calcareous primary producers must have caused major starvation higher up in the food chain. This would explain the extinctions of animals relying on plankton as their food source, the survival of organisms living in detritus-based food chains, and the dwarfing in evolutionary lineages observed in marine biota after the K-Pg boundary (*9*, *52*, *53*). The abrupt drop in plankton productivity was apparently short-lived as shown by marine biomarker data (*54*). The negative shift of the stable carbon isotopic value ($\delta^{13}C$) (Fig. 1) and the surface to deep water $\delta^{13}C$ gradient collapse is indicative of a major disruption to marine productivity and the ocean's biological pump (*11*). However, the large magnitude of the $\delta^{13}C$ anomaly suggests that the release of methane, input of soot, or the dependency of the isotopic signal on the metabolism of different species may have contributed to the anomaly (*50*).

On land, the loss of the diverse vegetation and the onset of the fern-spore spike following the K-Pg boundary indicates instantaneous (days to months) destruction of diverse forest communities coincident with deposition of ejecta from the Chicxulub impact (fig. S17) (*12*, *37*, *55*). A shutdown of photosynthesis because of low light levels is also indicated by high abundances of fungal spores in a thin layer of sediment preceding the recovery succession of ferns at a New Zealand K-Pg boundary site (*56*). Analogous to the marine environment, the abrupt elimination of the forest communities may have had similarly catastrophic effects on animals relying on primary producers (e.g., the herbivorous dinosaurs), whereas detritus-based food chains (e.g., in lakes) were apparently less affected (*52*).

Faunal and floral changes during the Late Cretaceous do occur [e.g., (*12*, *47*)] but are clearly distinguishable from the abrupt mass extinction and ecosystem disruption coincident with the K-Pg boundary, as indicated by high-resolution records of marine planktonic microfossils and terrestrial pollen and spores (*12*, *13*, *25*, *37*, *55*, *57*). Productivity proxies (e.g., carbonate content) linked to orbitally tuned stratigraphic time scales provide no evidence for major changes preceding the boundary (*39*). Claims of gradual or stepwise extinctions during the Late Cretaceous culminating in the K-Pg mass extinction (*14*) and survivorship through the K-Pg boundary may be explained by short-term survival with greatly reduced population sizes, sampling artifacts, or reworking of Cretaceous fossils [e.g., (*57*)]. In addition, the global onset of opportunistic species blooms and the evolutionary radiation of new taxa started consistently after the K-Pg boundary mass extinction (Fig. 1 and fig. S17) (*49*, *55*).

What Do We Need to Look at Next?

The correlation between impact-derived ejecta and paleontologically defined extinctions at multiple locations around the globe leads us to conclude that the Chicxulub impact triggered the mass extinction that marks the boundary between the Mesozoic and Cenozoic eras ~65.5 million years ago. This conclusion is reinforced by the agreement of ecological extinction patterns with modeled environmental perturbations. Although the relative importance of the different impact-induced environmental effects on the K-Pg mass extinction is still under scrutiny, alternative multi-impact or volcanic hypotheses fail to explain the geographic and stratigraphic distribution of ejecta and its composition, the timing of the mass extinction, and the scale of environmental changes required to cause it. Future geophysical, geological, and drilling studies of the Chicxulub structure will further constrain the impact process and the amount and nature of environment-altering gases generated by this so far unparalleled combination of a large impact into ~3- to 4-km-thick carbonate- and sulfate-rich target rocks. Research focused on high-resolution studies of the ejected material, integrated climate models, and detailed study of related fossil successions will help reveal the physical and biological mechanisms of the K-Pg mass extinction and may also aid in understanding other mass extinction events in Earth history.

References and Notes

1. J. Alroy, *Proc. Natl. Acad. Sci. U.S.A.* **105** (suppl. 1), 11536 (2008).
2. L. W. Alvarez, W. Alvarez, F. Asaro, H. V. Michel, *Science* **208**, 1095 (1980).
3. J. Smit, J. Hertogen, *Nature* **285**, 198 (1980).
4. A. Montanari *et al.*, *Geology* **11**, 668 (1983).
5. B. F. Bohor, *Tectonophysics* **171**, 359 (1990).
6. A. R. Hildebrand *et al.*, *Geology* **19**, 867 (1991).
7. O. B. Toon, K. Zahnle, D. Morrison, R. P. Turco, C. Covey, *Rev. Geophys.* **35**, 41 (1997).
8. E. Pierazzo, A. N. Hahmann, L. C. Sloan, *Astrobiology* **3**, 99 (2003).
9. D. A. Kring, *Palaeogeogr. Palaeoclimatol. Palaeoecol.* **255**, 4 (2007).
10. K. O. Pope, K. H. Baines, A. C. Ocampo, B. A. Ivanov, *J. Geophys. Res.* **102**, (E9), 21645 (1997).
11. S. D'Hondt, *Annu. Rev. Ecol. Evol. Syst.* **36**, 295 (2005).
12. A. R. Sweet, D. R. Braman, *Can. J. Earth Sci.* **38**, 249 (2001).
13. P. Bown, *Geology* **33**, 653 (2005).
14. G. Keller, W. Stinnesbeck, T. Adatte, D. Stüben, *Earth Sci. Rev.* **62**, 327 (2003).
15. S. Self, M. Widdowson, T. Thordarson, A. E. Jay, *Earth Planet. Sci. Lett.* **248**, 518 (2006).
16. A.-L. Chenet *et al.*, *J. Geophys. Res.* **114**, (B6), B06103 (2009).
17. J. Smit, *Annu. Rev. Earth Planet. Sci.* **27**, 75 (1999).
18. P. Claeys, W. Kiessling, W. Alvarez, *Spec. Pap. Geol. Soc. Am.* **356**, 55 (2002).
19. J. Urrutia-Fucugauchi, L. E. Marín, A. Trejo-Garcia, *Geophys. Res. Lett.* **23**, 1565 (1996).
20. I. Arenillas *et al.*, *Earth Planet. Sci. Lett.* **249**, 241 (2006).
21. K. Goto *et al.*, *Cretaceous Res.* **29**, 217 (2008).
22. J. Smit, W. Alvarez, A. Montanari, P. Claeys, J. M. Grajales-Nishimura, *Spec. Pap. Geol. Soc. Am.* **307**, 151 (1996).
23. P. Schulte, A. Kontny, *Spec. Pap. Geol. Soc. Am.* **384**, 191 (2005).
24. R. D. Norris, B. T. Huber, B. T. Self-Trail, *Geology* **27**, 419 (1999).
25. K. G. MacLeod, D. L. Whitney, B. T. Huber, C. Koeberl, *Geol. Soc. Am. Bull.* **119**, 101 (2007).
26. P. Schulte *et al.*, *Geochim. Cosmochim. Acta* **73**, 1180 (2009).
27. E. Molina *et al.*, *Episodes* **29**, 263 (2006).
28. J. V. Morgan *et al.*, *Earth Planet. Sci. Lett.* **251**, 264 (2006).
29. Materials and methods are available as supporting material on *Science* Online.
30. T. J. Bralower, C. K. Paull, R. M. Leckie, *Geology* **26**, 331 (1998).
31. G. Keller *et al.*, *Earth Planet. Sci. Lett.* **255**, 339 (2007).
32. G. Keller *et al.*, *Meteorit. Planet. Sci.* **39**, 1127 (2004).
33. L. Alegret, E. Molina, E. Thomas, *Geology* **29**, 891 (2001).
34. J. A. Arz, L. Alegret, I. Arenillas, *Meteorit. Planet. Sci.* **39**, 1099 (2004).
35. J. Smit, S. V. D. Gaast, W. Lustenhouwer, *Meteorit. Planet. Sci.* **39**, 1113 (2004).
36. T. J. Bralower *et al.*, *Geology*, in press.
37. D. J. Nichols, K. R. Johnson, *Plants and the K-T Boundary* (Cambridge Univ. Press, Cambridge, 2008), p. 280.
38. N. Robinson, G. Ravizza, R. Coccioni, B. Peucker-Ehrenbrink, R. D. Norris, *Earth Planet. Sci. Lett.* **281**, 159 (2009).
39. T. Westerhold *et al.*, *Palaeogeogr. Palaeoclimatol. Palaeoecol.* **257**, 377 (2008).
40. B. Ivanov, *Sol. Syst. Res.* **39**, 381 (2005).
41. N. Artemieva, J. Morgan, *Icarus* **201**, 768 (2009).
42. T. J. Goldin, H. J. Melosh, *Geology* **37**, 1135 (2009).
43. M. C. Harvey, S. C. Brassell, C. M. Belcher, A. Montanari, *Geology* **36**, 355 (2008).
44. K. O. Pope, *Geology* **30**, 99 (2002).
45. S. P. S. Gulick *et al.*, *Nat. Geosci.* **1**, 131 (2008).
46. T. Luder, W. Benz, T. F. Stocker, *J. Geophys. Res.* **108**, (E7), 5074 (2003).
47. P. Wilf, K. R. Johnson, B. T. Huber, *Proc. Natl. Acad. Sci. U.S.A.* **100**, 599 (2003).
48. D. E. Fastovsky, P. M. Sheehan, *GSA Today* **15**, 4 (2005).
49. I. Arenillas, J. A. Arz, E. Molina, C. Dupuis, *Micropaleontology* **46**, 31 (2000).
50. E. Thomas, *Spec. Pap. Geol. Soc. Am.* **424**, 1 (2007).
51. P. S. Willumsen, *Cretaceous Res.* **27**, 954 (2006).
52. P. M. Sheehan, P. J. Coorough, D. E. Fastovsky, *Spec. Pap. Geol. Soc. Am.* **307**, 477 (1996).
53. M. Aberhan, S. Weidemeyer, W. Kiessling, R. A. Scasso, F. A. Medina, *Geology* **35**, 227 (2007).
54. J. Sepúlveda, J. E. Wendler, R. E. Summons, K.-U. Hinrichs, *Science* **326**, 129 (2009).
55. V. Vajda, J. I. Raine, C. J. Hollis, *Science* **294**, 1700 (2001).
56. V. Vajda, S. McLoughlin, *Science* **303**, 1489 (2004).
57. C. R. C. Paul, *Palaeogeogr. Palaeoclimatol. Palaeoecol.* **224**, 291 (2005).

58. D.J.N. passed away during the final revision of this paper. His more than 30 years of work on the Cretaceous-Paleogene boundary influenced the data, ideas, and thesis of this paper. This research used samples and photos provided by the Ocean Drilling Program (ODP) and the International Continental Scientific Drilling Program (ICDP) and was funded by the Deutsche Forschungsgemeinschaft, the Austrian Science Foundation (FWF), Danish Carlsberg Foundation, European Social Fund, Research Foundation Flanders, Mexican Consejo Nacional de Ciencia y Tecnología, NASA, Japan Society for the Promotion of Science, Joint Oceanographic Institutions, K.U.Leuven Research Fund, UK Natural Environment Research Council, NSF, the Swedish Research Council (VR) and the Royal Swedish Academy of Sciences through the Knut and Alice Wallenberg Foundation, and the Spanish Ministerio de Ciencia e Innovación. We are grateful to E. Thomas and an anonymous reviewer for valuable comments and thank G. Izett for providing support and photos.

Supporting Online Material

www.sciencemag.org/cgi/content/full/327/5970/1214/DC1
Materials and Methods
SOM Text
Figs. S1 to S17
Tables S1 to S3
References

10.1126/science.1177265